Diffusion of Knotted DNA Molecules in Nanochannels in the Extended de Gennes Regime

Zixue Ma and Kevin D. Dorfman*

Department of Chemical Engineering and Materials Science, University of Minnesota – Twin Cities, 421 Washington Ave SE, Minneapolis, Minnesota 55455, USA

E-mail: dorfman@umn.edu

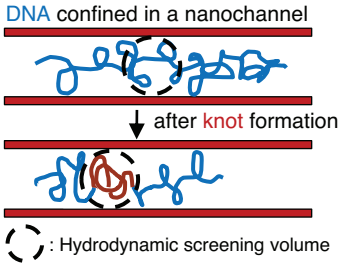

Abstract

We study the diffusion of T4 GT7 deoxyribonucleic acid (DNA) molecules confined in nanochannels with an effective size of 307 nm before and after knot formation. The measured DNA chain diffusivity is 0.0243 ± 0.0009 $\mu m^2/s$ for unknotted DNA molecules, and 0.014 ± 0.001 $\mu m^2/s$ for the DNA containing knots with an estimated knot contour length of 9 ± 2 μm. The reduced diffusivity in the presence of large knots indicates that the DNA-wall friction, rather than the shortening of the non-draining molecule, dominates the friction of knotted DNA in the extended de Gennes regime of nanochannel confinement.

1 Introduction

Long polymers such as deoxyribonucleic acid (DNA) are likely to self-entangle into knots.[1–3] This topological object affects the mechanical and dynamical properties of the polymers;[3,4] in particular, the presence of knots increases the mobility of the polymer chain in free solution.[5–7] The corresponding effect of knot formation on diffusion of DNA confined in nanochannels, however, remains an open question.

Unknotted DNA under the weak confinement conditions considered here is described by blob theory,[8] with a friction that is proportional to the extension of the polymer along the channel axis.[9] In other words, the confined DNA is a non-draining object. Two competing factors are expected to change the DNA friction, which is inverse to the diffusivity, due to the presence of a knot. The formation of a knot in a DNA molecule decreases the extension of the confined molecule as illustrated in Figure 1, thus decreasing the friction of the non-draining object by reducing its size. A potential counteracting effect is the increased friction between the knotted part of the DNA chain and the nanochannel surface. The DNA knot fills the hydrodynamic screening volume in a more compact way, giving rise to the DNA chain closer to the channel wall as shown in Figure 1b and increases DNA-wall friction. It is not obvious, *a priori*, which of these competing mechanisms is more important.

Here we measured the center-of-mass diffusivity of T4 DNA molecules confined in nanochannels with an effective size of 307 nm before and after knot formation to address which of these competing effects dominates knotted DNA diffusion in the extended de Gennes regime, i.e., for channel sizes that lie between the Kuhn length and thermal blob size of the DNA.[10] The diffusivity scaling of semiflexible polymers under the extended de Gennes regime in nanochannel confinement is described by a modified blob theory which incorporates the effect of local chain stiffness.[11–13] In this confinement regime, the polymer chain remains a non-draining object with a small correction due to the stiffness of the chain.[11,12] We use a nanofluidic "knot factory" device introduced by Amin *et al.*[14] for efficient large knot generation. The knot factory device consists of nanochannels with nanoslits that enables us

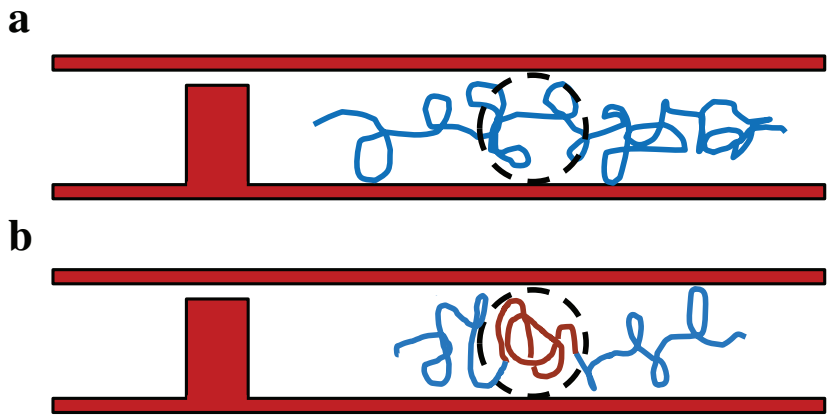

Figure 1: Schematic illustration of a cross-sectional view of a DNA molecule confined in a nanochannel (340 nm deep) with a 32 nm deep nanoslit (not to scale) before and after knot formation in the chain. (a) A single DNA chain (blue curve) confined in a nanochannel before being compressed against a nanoslit for knot generation. (b) A knot shown in red is formed along the DNA chain (blue curve). The black dashed line represents the screening volume of hydrodynamic interactions.

to use a pressure-driven flow to compress the DNA against the nanoslits to generate knots efficiently. T4 DNA molecules are chosen as the model system due to their higher molecular weight relative to the other standard model system, λ-DNA. Such long T4 DNA chains lead to a higher probability of knot formation[15,16] and a longer diffusion time of knots along the DNA chains,[17,18] which allows us to have sufficient time to investigate the knotted DNA diffusion before the knots unravel at the end of the chains. Our results show that the presence of knots decreases the DNA chain diffusivity in nanochannels, which demonstrates that the increase in DNA-wall friction dominates the reduction in chain extension for the knotted DNA chain diffusion under the extended de Gennes regime in nanochannel confinement.

2 Experimental Methods

2.1 Device fabrication

The nanochannel devices designed based on the concept of the knot factory[14] were fabricated on fused silica substrates (University Wafers) by a combination of electron beam lithography and photolithography followed by a fluorine (CF_4:CHF_3) reactive ion etching step as described in Ref. 18. The nanofluidic device consists of two U-shaped microchannels (50 μm wide, 0.8 μm deep) with an arm length of 8 mm adjoining the reservoirs and the nanochannles with height, D_1, of 340 nm and width, D_2, of 304 nm. The nanochannels are 450 μm long with nanoslits (500 nm wide, 32 nm deep) in the channel centers. A cross-sectional view of a nanochannel at the device center with a nanoslit is shown in Figure 1. Additional details of the device fabrication and design are reported in Ref. 18.

2.2 DNA diffusion experiments

The nanofluidic device was filled with a DNA sample solution by capillary action. The solution contains 0.25× TBE buffer, β-mercaptoethanol (Sigma-Aldrich, 4% v/v) to suppress photobleaching, and T4 GT7 DNA molecules (166 kilobase pairs, Nippon Gene) stained with YOYO-1 fluorescent dye (Invitrogen) at a dye to DNA base pair ratio of 1:10, resulting in a contour length, L, of 65 μm.[19,20] The ionic strength of this solution is 18 mM, calculated following a previous approach.[21,22] The wet device was assembled into a chuck with inlets that allow for applying pressure.[21,23] The pressure was controlled using a microfluidic flow control system (Fluigent MFCS-EZ). Following the loading of the DNA solution, 6 μL of buffer solution with the same ionic strength as the DNA sample solution was subsequently added to each port of the chuck, linked to the reservoirs on the nanofluidic device, to prevent fluid flow through channels. The chuck was then mounted on an inverted epifluorescene microscope (Olympus IX73) with a 100× (1.4 N.A.) oil immersion objective. Imaging of DNA diffusion before and after compression was performed using a blue laser (Coherent

OBIS, 473 nm) with a power of 1 mW and an EMCCD camera (Photometrics, Cascade II:512) at 2 fps with a 200 ms exposure time for 1000 s. The compression step for knot generation was conducted using the method described in Ref. 18. After the experiment, the device was cleaned and dried to allow it to be reused for the next experiment.[18]

2.3 Data processing

The movies of DNA molecules in nanochannels were analyzed using a custom-written MATLAB program.[24] The positions of the edges of the DNA molecules, $x_1(t)$ and $x_2(t)$, were extracted by fitting the intensity profile, $I(x,t)$, to a convolution of a box function with a Gaussian point-spread function.[25] The intensity-weighted center of mass of the DNA molecules,[12,26] $x_{\rm com}(t)$, was then calculated as

$$x_{\rm com}(t) = \frac{\int_{x_1(t)}^{x_2(t)} xI(x,t)\,dx}{\int_{x_1(t)}^{x_2(t)} I(x,t)\,dx} \tag{1}$$

In the experiment, we measured the center of mass motion for individual DNA molecules over a relatively short time due to unknotting of DNA molecules, stage drift and photocleavage of YOYO-stained DNA in long exposure times.[27] The motion of a single DNA molecule provides a measurement of the time-averaged mean-squared displacement (MSD) with localization errors under a particular configuration, which does not provide sufficient statistics to obtain the long-time chain diffusivity. To sample molecules with diverse configurations, an ensemble of DNA molecules is required to calculate the ensemble-averaged MSD with standard errors as measured over the ensemble of molecules. The time evolution of the center of mass, $x_{\rm com}(t)$, was used to compute the ensemble-averaged MSD

$$\mathrm{MSD}(\delta t) = \left\langle [x_{\rm com}(t) - x_{\rm com}(t-\delta t)]^2 \right\rangle_{\rm t,n} \tag{2}$$

where $\langle \ldots \rangle_{\rm t,n}$ denotes an average over all times t and the ensemble of n DNA molecules, and

δt is the time lag between images.[12] A time-averaged MSD was also calculated using Eq. 2 without averaging over n to show each DNA molecule's trajectory.

In the experiment, the DNA molecules are susceptible to drift towards one direction caused by a pressure drop from unequal fluid levels in reservoirs.[12,26] To ensure that measurements are free of this artifact, we performed an analysis to detect the systematic errors due to DNA drift in nanochannels. First, we computed the scaling exponent β of the ensemble-averaged MSD for DNA molecules in each video by fitting the logarithm of the data with a linear function

$$\log_{10} \mathrm{MSD}(\delta t) = \beta \log_{10} \delta t + c_\beta \tag{3}$$

following the method from York,[28] where c_β is a fitted constant. We also calculated the cross correlation coefficient, $C_{A,B}$ between DNA molecules A and B in a given video

$$\mathrm{C_{A,B}} = \frac{\left\langle [x_{\mathrm{com,A}}(t) - \langle x_{\mathrm{com,A}}(t) \rangle_{\mathrm{t}}][x_{\mathrm{com,B}}(t) - \langle x_{\mathrm{com,B}}(t) \rangle_{\mathrm{t}}] \right\rangle_{\mathrm{t}}}{\sigma_{\mathrm{x_{com,A}}} \sigma_{\mathrm{x_{com,B}}}} \tag{4}$$

where $x_{\mathrm{com,A}}(t)$ and $x_{\mathrm{com,B}}(t)$ are the centers of mass of different DNA molecules at time t, and $\sigma_{\mathrm{x_{com,A}}}$ and $\sigma_{\mathrm{x_{com,B}}}$ are their standard deviations. We then define an overall correlation coefficient for an ensemble of molecules in each movie, denoted as C, that is computed as the average of $C_{A,B}$ obtained for all possible molecules in the movie; if each molecule is highly cross-correlated with every other molecule in its movie, this is indicative of a fluid flow. A k-means clustering analysis partitioned the data for β and C into three clusters as shown in Figure S1. The cluster with high β and C values are highly correlated DNA molecules with superdiffusive behavior, consistent with the effect of fluid flow. These molecules were excluded from the subsequent analysis.

The DNA chain diffusivity, D, was then obtained by fitting the ensemble-averaged MSD

data of the non-drifting DNA molecules with a linear function

$$\mathrm{MSD}(\delta t) = 2D\delta t + c_{\mathrm{D}} \tag{5}$$

using the least-squares fitting method from York,[28] where c_{D} is a fitted constant. The ensemble-averaged MSD of unknotted DNA molecules was fit from 50 to 227 s to extract the diffusivity of DNA before compression. For the knotted DNA molecules, their ensemble-averaged MSD data was fit from 200 to 418 s. The lower and upper bounds for fitting the data were determined using the method described previously.[18] The details of determination of the bounds are shown in Figure S2.

3 Results

The modified blob theory applies to the polymer chains under the extended de Gennes regime in nanochannel confinement.[11,12] A necessary step before the analysis of T4 DNA diffusion in nanochannels is to confirm that our experiments of confined DNA are located in the extended de Gennes regime. We thus calculate the effective channel size D_{eff}, using the equation $D_{\mathrm{eff}} = \sqrt{(D_1 - \delta)(D_2 - \delta)}$. The wall depletion length, δ, is an offset to account for the DNA-wall excluded volume and electrostatic interactions,[12,29,30] which is computed to be 14 nm in our experiments using the model developed by Bhandari *et al.*[29] The effective channel size of our nanochannels is 307 nm, which is in the extended de Gennes regime boundaries of 241 and 694 nm as determined by simulations.[31] We also confirm that our measured average extension of stained T4 DNA molecules is consistent with the theoretically predicted extension of nanochannel confined T4 DNA in the extended de Gennes regime. The fractional extension of semiflexible polymers in the extended de Gennes regime is predicted to be 0.23 for our effective channel size,[32] corresponding to an extension of 15 μm for intact, stained T4 DNA molecules with a contour length of 65 μm.[19,20] The measured average extension estimated from uncorrelated measurements of the extensions of T4 DNA molecules

before knotting is 14.8 μm with a standard error of 0.3 μm, within experimental error of the predicted value of 15 μm.

The stained T4 DNA with a contour length of about 65 μm[19,20] are long DNA molecules. Thus, the molecules are susceptible to breakage by hydrodynamic forces when being compressed against nanoslits for knot generation.[33] To confirm that the shortening of knotted DNA is due to knot formation, we examine T4 DNA molecules without knot generation from the compression process to study whether T4 DNA are sheared after being compressed against nanoslits. An unpaired two-sample t-test at a 5% significance level was used to compare the average extension of 10 molecules that do not form knots before and after the compression step. The test results show that three molecules are rejected in the hypothesis test, but the change in average extension of those rejected molecules is 0.4 μm with a standard error of 0.03 μm. This small value relative to the average extension of T4 DNA suggests that the T4 DNA molecules are not significantly shortened after the compression step, consistent with the experimental result from our previous work.[18] As a consequence, our experimental results lead to a conclusion that the measured T4 DNA molecules for diffusion analysis are intact. The observed shortening of 2 μm, with a standard error of 0.5 μm, for the knotted DNA after being compressed against nanoslits is thus due to knot formation, not any shearing due to the compression process. The knot contour length is estimated to be 9 μm with a standard error of 2 μm, computed from the reduced extension and a theoretically predicted fractional extension of 0.23.[32]

Figure 2 provides an example of a single T4 DNA diffusing in a nanochannel before and after a knot, observed as a bright spot in Figure 2c, is formed in the chain. In the kymograph of the knotted DNA as seen in Figure 2c, the bright streak is the trajectory of the knot moving along the DNA chain. Such a bright feature is associated with a knot because knots are persistent and can only unravel at the end of a chain, which is different from other topological events such as folds.[14,17,18,34–36] Folded configurations also occur in our experiments during injection of the DNA into the nanochannels,[34,35] but the molecules

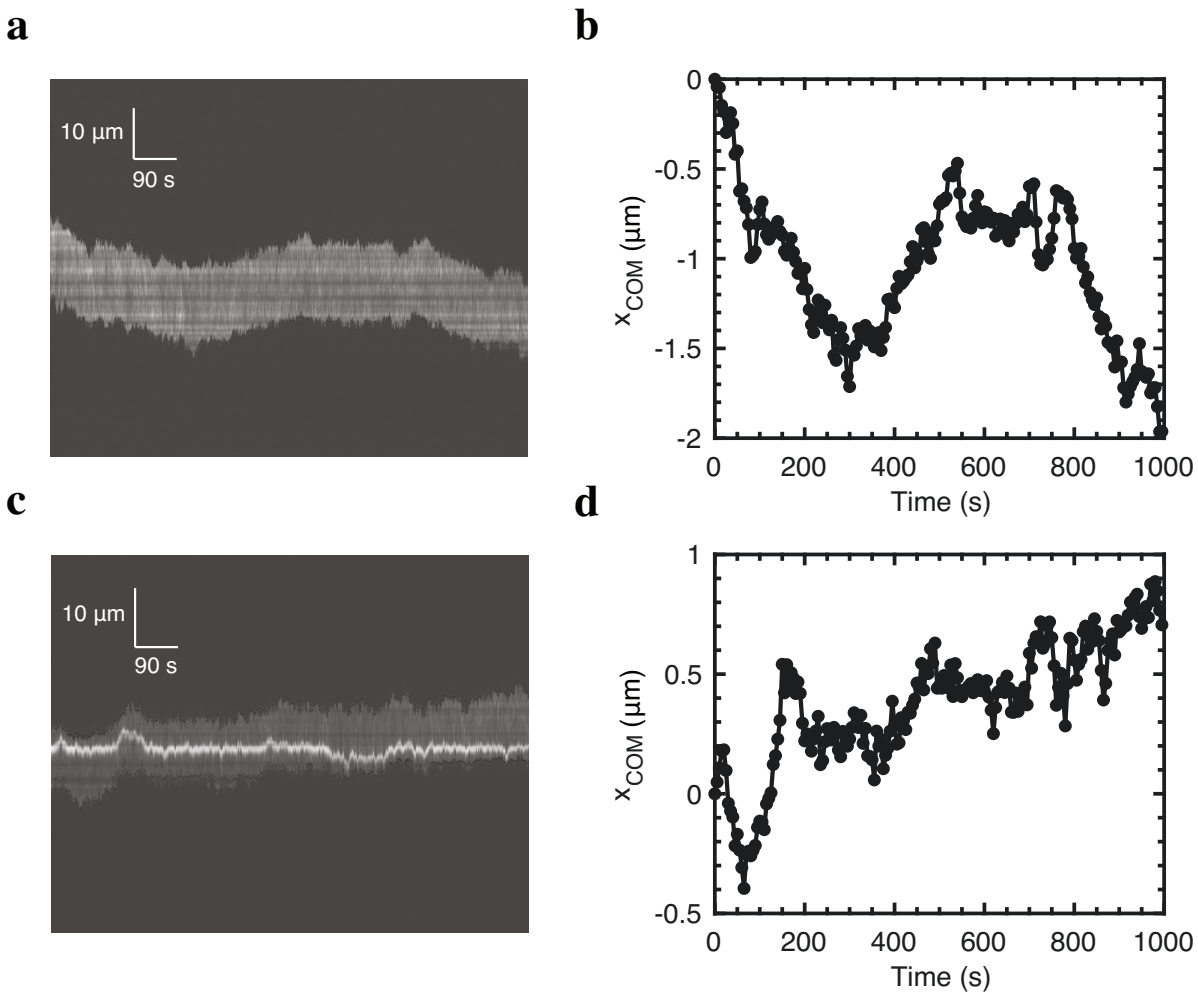

Figure 2: Trajectory of a single T4 DNA confined in a nanochannel before and after a knot was generated in the DNA chain. (a, c) Kymograph and (b, d) time evolution of the intensity-weighted center of mass for an unknotted T4 DNA (a, b) and a T4 knotted DNA (c, d) confined in a nanochannel. In the kymographs, the vertical axis is the intensity along the nanochannel and the horizontal axis is the time. The knot is identified as a bright spot. Black dots superimposed on the ends of the DNA are produced by the imaging processing code to locate the DNA.

unfold before the start of image acquisition. In addition, we produce the time evolution of the intensity-weighted center of mass for the unknotted (Figure 2b) and knotted DNA molecule (Figure 2d) by processing the kymographs.

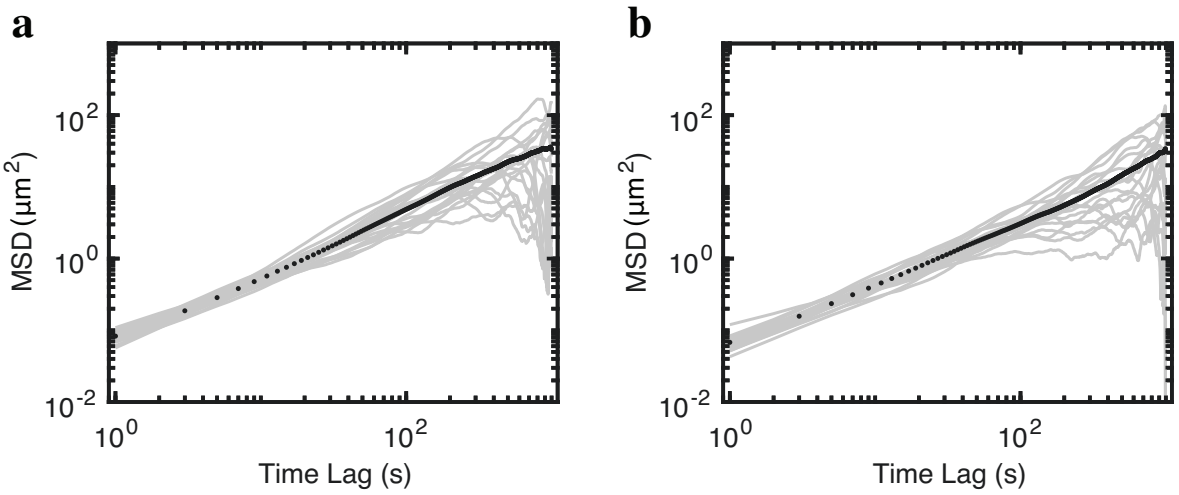

Figure 3: A log-log plot of mean-squared displacement (MSD) of 20 T4 DNA confined in nanochannels as a function of time lag. (a) The time-averaged MSDs (gray lines) and the ensemble-averaged MSD (black dots) of T4 DNA molecules before compression as a function of time lag. The scaling exponent, β, extracted by fitting the ensemble-averaged MSD data for $\delta t \in$ [50 s, 227 s] is 1.00 ± 0.03. (b) T4 DNA molecules with knots, same type of plot as in panel a. The β value obtained by fitting the ensemble-averaged MSD curve for $\delta t \in$ [200 s, 418 s] is 1.0 ± 0.1. The errors are calculated using 95% confidence interval.

Figure 3 shows the time-averaged MSDs computed from the time evolution of center of mass of 20 molecules along with the ensemble-averaged MSD as a function of time lag for the measured T4 DNA molecules before and after knot formation. The ensemble-averaged MSD allows us to obtain the diffusivity of DNA chain confined in nanochannels. One potential systematic error in the measurement of DNA diffusivity is anomalous diffusive behavior of DNA molecules due to induced motion of DNA by fluid flow or adsorption of DNA onto nanochannel surface.[12] We already performed a k-means clustering analysis to identify correlated, superdiffusive molecules due to flow. To confirm that our data set is indeed free of this artifact, we computed the scaling exponent β of the ensemble-averaged MSD before and after knotting for the molecules that were not removed by the k-means clustering. Fitting

of the linear function Eq. 3 to the logarithm of the ensemble-averaged MSD yields a scaling exponent of 1.00 ± 0.03 for DNA molecules before compression and a scaling exponent of 1.0 ± 0.1 for the DNA with knots after being compressed against nanoslits at a 95% confidence level. Both values of the scaling exponent at 95% confidence indicate a normal diffusive behavior of the observed DNA molecules before and after knot generation.

We thus proceed to investigate the effect of knots on the DNA chain diffusion by comparing the diffusivity of DNA molecules before and after knots are formed along the DNA chains. Figure 4 shows the ensemble-averaged MSD as a function of time lag and the linear fits to the data for observed DNA molecules before and after knot generation. The diffusivity for the unknotted DNA chains is 0.0243 ± 0.0009 $\mu m^2/s$ by fitting the ensemble-averaged MSD curve between 50 and 227 s. For the DNA containing knots, the ensemble-averaged MSD was fit from 200 to 418 s to extract the diffusivity value which is 0.014 ± 0.001 $\mu m^2/s$. Note that the errors are calculated using a 95% confidence interval. The diffusion constant of the knotted DNA molecules is smaller than the value of the DNA without knots. The result indicates that the formation of knots decreases the diffusivity of DNA chain in the extended de Gennes regime.

Two potential sources of systematic error in the measurement of knotted DNA diffusivity in nanochannels are that (i) the knot factory device produces knots with varying sizes and (ii) multiple knots can be generated along a T4 DNA chain. Examples of both effects are shown in Figure 5. Figure 6 illustrates the relationship between knotted DNA chain diffusivity and knot contour length for the 20 measured knotted T4 DNA molecules. The knotted DNA chain diffusivity decreases as the knot contour length increases. This result supports our claim that the presence of knots decreases the DNA chain diffusivity in nanochannels in the extended de Gennes regime. The number of knots in a DNA molecule may also affect the knotted DNA chain diffusivity. We observed that two of the 20 measured T4 DNA molecules formed two knots. The chain diffusivity of one molecule containing two knots with a contour length of 4.7 ± 0.6 μm is 0.0224 ± 0.0002 $\mu m^2/s$, which is larger than the averaged chain

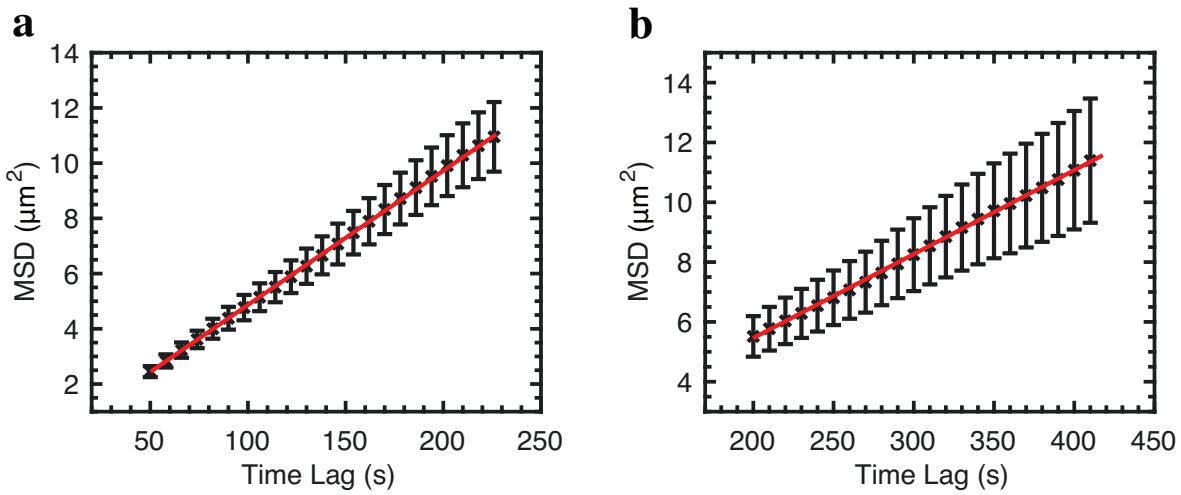

Figure 4: Ensemble-averaged MSDs of 20 measured T4 DNA molecules before and after knot formation as a function of time lag. (a) The ensemble-averaged MSD of unknotted DNA molecules was fit to a linear line (solid red line) for $\delta t \in [50\text{ s}, 227\text{ s}]$ to extract the diffusivity which is $0.0243 \pm 0.0009\ \mu\text{m}^2/\text{s}$. (b) A linear fit (solid red line) to the ensemble-averaged MSD data of knotted DNA in nanochannels for $\delta t \in [200\text{ s}, 418\text{ s}]$ yields a diffusivity value of $0.014 \pm 0.001\ \mu\text{m}^2/\text{s}$. The errors in the linear regression are estimated using a 95% confidence interval. Error on the ensemble-averaged MSD for a given time lag is the standard error.

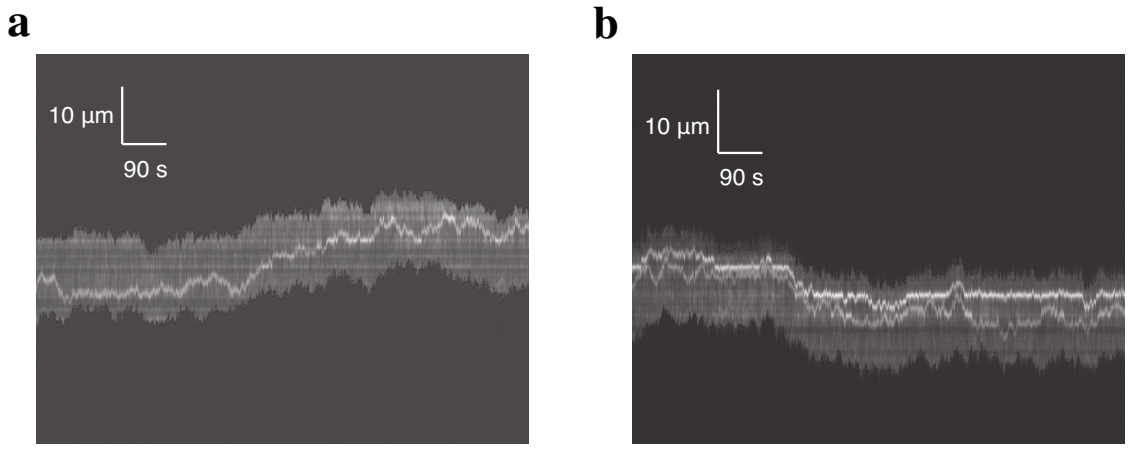

Figure 5: Examples of kymographs for (a) a knotted T4 DNA molecule with a smaller knot compared with the molecule in Figure 2c and (b) a knotted T4 DNA molecule with two knots formed in the chain. The intensity along the nanochannel (vertical axis) is plotted versus time (horizontal axis). Knots are visualized as bright spots along the DNA chains. Black dots at the ends of DNA chains are created by the image processing code to locate the DNA molecule.

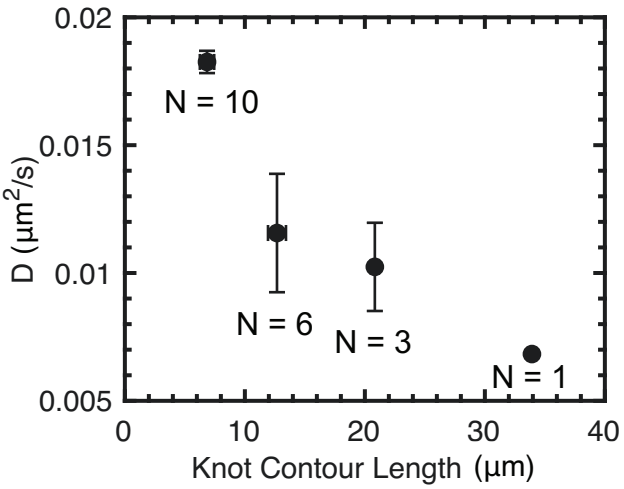

Figure 6: The knotted DNA chain diffusivity as a function of knot contour length. The N value represents the ensemble size of knotted T4 DNA molecules for calculating the knotted DNA chain diffusivity. Errors on the knotted DNA chain diffusivity are calculated using 95% confidence interval. Error bar on the knot contour length represents the standard error as measured over multiple knotted DNA molecules. The uncertainty is not estimated for the point with N = 1 due to insufficient number of molecules with such large knot contour length of 34 μm.

diffusivity of 0.0163 ± 0.0003 μm^2/s for molecules containing a single knot with a contour length of 5.2 ± 0.3 μm. However, the chain diffusivity of 0.0127 ± 0.0002 μm^2/s for the other molecule involving two knots with a contour length of 9.9 ± 0.7 μm is within the uncertainty of the DNA chain diffusivity of 0.015 ± 0.003 μm^2/s for molecules containing a single knot with a knot contour length of 10.3 ± 0.5 μm. The experimental result is inconclusive for the effect of knot number on knotted DNA chain diffusivity due to insufficient data because, even though the center-of-mass errors are small, adequate sampling of the full configuration space requires observing more molecules since long tracks are not possible.

4 Discussion

We observed the T4 DNA diffusion in nanochannels before and after knot formation to study the effect of knots on the DNA chain diffusion under the extended de Genne regime in nanochannel confinement. The DNA chain diffusivity is found to be 0.0243 ± 0.0009 μm^2/s

for T4 DNA molecules without knots. The measured unknotted T4 DNA chain diffusivity is in good agreement with the value predicted by the modified blob theory that incorporates the effect of local stiffness of chains on semiflexible polymer diffusion in nanochannels.[11,12] Gupta *et al.*[12] measured the diffusivity of λ-DNA in nanochannels with effective sizes from 117 to 260 nm and obtained the coefficients of the modified blob theory model by fitting the experimental data. The value of T4 DNA diffusivity in nanochannels predicted using the modified blob theory model from Gupta *et al.*[12] is 0.023 ± 0.006 $\mu m^2/s$. Companion simulations of the Kirkwood diffusivity of nanochannel confined, long semiflexible chains suggest that the diffusivity of T4 DNA chain confined in our nanochannels is 0.022 ± 0.003 $\mu m^2/s$.[11,12] Note that these values are computed using a fractional extension of 0.23 predicted by a model for semiflexible polymers in the extended de Gennes regime[32] and a Rouse diffusivity of 0.00377 $\mu m^2/s$ for T4 DNA with a contour length of 65 μm in water at room temperature of 25 °C.[12] Our experimentally measured diffusivity of unknotted T4 DNA in nanochannels is close to the predicted values from both previous experiments and simulations.

The T4 DNA chain diffusivity is decreased to 0.014 ± 0.001 $\mu m^2/s$ after knots are generated in the molecules. The decrease in the chain diffusivity of nanochannel confined DNA molecules after knot formation reveals that the DNA-wall friction dominates the knotted DNA diffusion in the extended de Gennes regime. The presence of knots decreases the size of DNA molecules in nanochannel confinement, thus decreasing the friction of the DNA chains. The knots, however, fill the screening volume of hydrodynamic interactions more densely, leading parts of the DNA chain to be closer to the channel surface. Thus, the friction between the DNA chain and channel wall is increased, more than counteracting the effect of decreased DNA size.

The formation of a knot, on average, increases the DNA friction by a factor of 1.7. To determine if this increase is consistent with increased DNA-wall friction due the knot, let us consider a simple model where the total friction consists of the sum of two components: (i) the friction due to the unknotted portion of the confined DNA molecule and (ii) the

friction due to a tight knot.[37] For the first contribution, we assume that the friction due to the unknotted part of the DNA is proportional to the knotted DNA extension X_k in the channel, consistent with the non-draining hydrodynamics in the extended de Gennes regime.[11] This assumption requires that the knotted part of the DNA chain is small so that it does not contribute to the total extension of the knotted DNA chain. For the second contribution, we model the hydrodynamics of the knot as a solid object of radius a confined in a cylindrical channel of diameter $R = \sqrt{D_1 D_2}/2$, corresponding to a channel radius of 161 nm. While this is a crude approximation for the hydrodynamics, it permits a closed form solution. Explicitly, for a closely fitting sphere, the average friction is approximately $6\pi\eta a(R/a-1)^{-5/2}$, where $\eta = 0.89$ cP is the viscosity of water at room temperature.[38] The sum of these two frictions, which is the total friction of knotted DNA, is thus

$$\xi_k = \hat{\xi}_0 X_k + 6\pi\eta a(R/a-1)^{-5/2} \tag{6}$$

where $\hat{\xi}_0 = 11.4$ cP is the friction per unit length of unknotted DNA, obtained from the diffusion data in Figure 4 using $X_u = 14.8$ μm as the average extension of an unknotted chain. The corresponding friction of an unknotted molecule is $\xi_u = \hat{\xi}_0 X_u$. As a result, the ratio of the friction coefficients is

$$\frac{\xi_k}{\xi_u} = \frac{X_k}{X_u} + \frac{6\pi\eta a}{\hat{\xi}_0 X_u (R/a-1)^{5/2}}. \tag{7}$$

The first term in Eq. 7, $X_k/X_u = 0.86$, quantifies the reduction in friction due to the shortening of the DNA molecule to $X_k = 12.8$ μm, while the second term in Eq. 7 quantifies the increase in friction due to knot formation. To be consistent with the experimental result $\xi_k/\xi_u = 1.7$, the hydrodynamic size of the knot needs to be $a = 135$ nm, i.e. the knot fills 84% of the channel volume. The knot in this model is small, which justifies the assumption that the friction due to the unknotted part of the DNA molecule is proportional to X_k.

Clearly this model is very simplistic in its treatment of the hydrodynamics. First, de-

coupling the two contributions to the friction is partially justified by the screening of hydrodynamic interactions at the length scale of the channel,[9] but the friction of the knot itself is not quantitatively equivalent to that of a solid sphere. Nevertheless, the arguments made in the context of Eq. 7 support the key point of our argument; the formation of a tight knot that fills a significant fraction of the channel size can easily reduce the overall friction two-fold. Second, it is unlikely that the knot can be actually as tight as predicted from this hydrodynamic model (even after accounting for the differences between the radius of gyration and hydrodynamic radius); if the knot were completely dry, its radius $R_g \approx bN^{1/3}$ is around 400 nm based on a Kuhn length $b = 100$ nm and the estimated knot contour length of 9 μm. It is more plausible that the confined knot is an anisotropic, extended object[39] that does not fill the channel as densely as anticipated by our simple model. The details of the knot conformation do not undermine our key idea; this extended knot configuration would still increase DNA friction because the friction increases quickly as the size of the object increases.[38] A detailed understanding of the hydrodynamics of confined knots that leverages tools for computing DNA-wall hydrodynamics,[11,40,41] is a promising avenue for future computational work.

Our hypothesis for the knotted DNA diffusion in nanochannels is that the dominant contribution to the DNA motion in nanochannels is the moving DNA with a fixed knot ball in the chain which provides extra friction between the knot and channel wall. The model does not consider knot transport as significant contribution to the knotted DNA chain diffusion. An alternative hypothesis is that the motion of knotted DNA in nanochannels is driven by knot self-reptation along the DNA chain without any superimposed motion of the whole polymer. We thus performed two analyses, one investigating the correlation between center of mass motion of DNA and the motion of the knot within the molecule and the other measuring the magnitude of the knot contribution to the center of mass motion of DNA molecules, to test this hypothesis. The first analysis we performed was to calculate the Pearson correlation coefficient between knot motion relative to one of the DNA chain ends

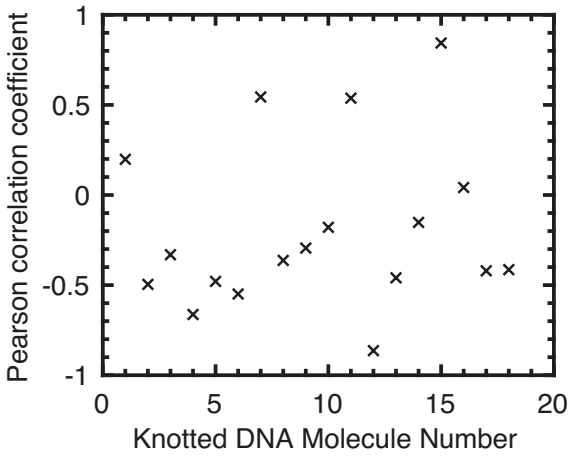

Figure 7: Scatter plot of Pearson correlation coefficient between knot motion relative to one of DNA chain ends and center of mass motion of DNA for 18 observed T4 DNA molecules that each contain a single knot. The negative correlation coefficient indicates that the knot moves along the DNA chain in an opposite direction of DNA motion in a nanochannel.

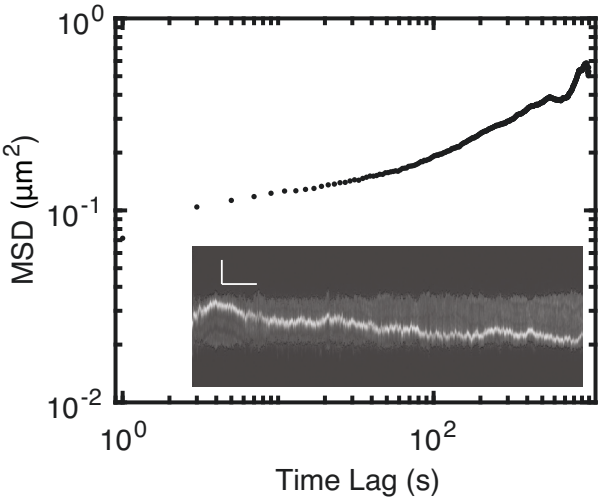

Figure 8: A log-log plot of ensemble averaged mean-squared displacement (MSD) as a function of time lag for 20 knotted T4 DNA molecules in nanochannels after shift of positions. The inset shows an example of a kymograph for a knotted DNA in Figure 2c after the position of the molecule in each frame is shifted to keep a constant center. The vertical axis is the intensity along the nanochannel with a scale bar of 5 μm and the horizontal axis is the time with a scale bar of 90 s.

and center of mass motion of DNA for 18 knotted DNA molecules that contain a single knot each. Figure 7 shows that the knot motion and DNA center of mass motion are negatively correlated for 13 of the knotted DNA molecules, consistent with the knot self-reptation model that the knot tends to move in an opposite direction of the DNA motion, but there is no strong correlation between the motion of knot and center of mass motion of knotted DNA molecules. We then measured the magnitude of the knot contribution to the center of mass motion of knotted DNA molecules. To do so, we centered each knotted DNA molecule in each frame within the same movie. An example of a centered DNA molecule is shown in Figure 8. Then, we calculated the intensity weighted center of mass of each fixed DNA molecules. Figure 8 shows the ensemble-averaged MSD as a function of time lag of the 20 knotted T4 DNA molecules using the center of mass of fixed knotted DNA chains. The ensemble-averaged MSD caused by motion of the knot along the chain contour is two orders of magnitude smaller than the ensemble-averaged MSD of moving DNA molecules with knots shown in Figure 3b. The results from two analyses indicate that the knot contributes to the knotted DNA in a manner consistent with self-reptation, but the contribution from knot movement to the knotted DNA diffusion in nanochannels is not significant compared with that from the whole chain motion.

The results of decreased chain diffusivity of knotted DNA confined in nanochannels contrast with the free solution data of Kanaeda and Deguchi,[5] who found that the ratio of diffusion constants for knotted ring polymers and a linear polymer with the same molecular weight in good solvent increases linearly with the average crossing number of knots, thus suggesting polymers with knots move faster. This discrepancy is plausibly due to the difference in the knot size and topological complexity of knots. They studied simpler small knots with seven crossings and fewer.[5] The topology of knots generated in our experiments cannot be identified through images, but the knots contain a contour length of 9 ± 2 μm, which is an order of magnitude larger than the size of simple knots with several hundreds nanometers of length.[36] The inconsistency may also be attributed to the absence of polymer-wall friction

in free solution. The presence of knots simply reduces the size of the non-draining objects, giving rise to a decreased friction of the object and a resulting increased mobility of the knotted ring polymers in a good solvent.

5 Conclusion

We have examined the diffusion of T4 DNA molecules in nanochannels before and after knot formation. The chain diffusivity of knotted T4 DNA molecules confined in nanochannels is found to be 0.014 ± 0.001 $\mu m^2/s$, which is smaller than the measured diffusivity of 0.0243 ± 0.0009 $\mu m^2/s$ for the T4 DNA molecules before knot generation. Our experimental results reveal that the presence of knots decreases the chain diffusivity of DNA molecules in nanochannels, indicating that the DNA-wall friction dominates knotted DNA diffusion under the extedned de Gennes regime in nanochannel confinement.

While our observation of diffusion of DNA with large knots with an estimated contour length of 9 ± 2 μm indicates that the knots decrease the DNA chain diffusivity in the extended de Gennes regime, a complete understanding of the effect of knot formation on DNA chain diffusion requires a study of diffusion of DNA chain with small knots as well in the confinement regime. Such experiments for probing the diffusion of DNA with small knots are challenging, in terms of identification of small knots using fluorescence microscopy and long duration of image acquisition of small knots, which will move faster along DNA chains.[36] Computational studies, alternatively, could provide insight into the effect of small knots on the DNA chain diffusivity in the extended de Gennes regime because it should be relatively straightforward to precondition the system to a particular knot size. The effect of knot type on DNA chain diffusion is also an intriguing question for theoretical studies because identifying the topology of knots is considerably more straightforward in a simulation than in experiments.[42–48] Other open questions related with the effect of knots on DNA chain diffusivity in nanochannels also remain, particularly the effect of multiple knots, a more

complex and intriguing phenomenon.

Acknowledgement

This work was supported by NSF (CBET-2016879). Device fabrication was conducted in the Minnesota Nano Center, which is supported by the National Science Foundation through the National Nano Coordinated Infrastructure Network (NNCI) under Award Number ECCS-2025124.

Supporting Information

k-means clustering analysis, and determination of upper and lower bounds of the time lag used for fitting the DNA chain diffusivity

References

(1) Liu, L. F.; Perkocha, L.; Calendar, R.; Wang, J. C. Knotted DNA from bacteriophage capsids. *Proc. Natl. Acad. Sci. U.S.A.* **1981**, *78*, 5498–5502.

(2) Rybenkov, V. V.; Cozzarelli, N. R.; Vologodskii, A. V. Probability of DNA knotting and the effective diameter of the DNA double helix. *Proc. Natl. Acad. Sci. U.S.A.* **1993**, *90*, 5307–5311.

(3) Meluzzi, D.; Smith, D. E.; Arya, G. Biophysics of knotting. *Annu. Rev. Biophys.* **2010**, *39*, 349–366.

(4) Orlandini, E. Statics and dynamics of DNA knotting. *J. Phys. A: Math. Theor.* **2018**, *51*, 053001.

(5) Kanaeda, N.; Deguchi, T. Universality in the diffusion of knots. *Phys. Rev. E* **2009**, *79*, 021806.

(6) Matuschek, D. W.; Blumen, A. Increase of the mobility of knotted macromolecules. *Macromolecules* **1989**, *22*, 1490–1491.

(7) Croxton, C. A.; Turner, R. M. Iterative convolution determination of the mobility of knotted macromolecules. *Macromolecules* **1991**, *24*, 177–183.

(8) Daoud, M.; de Gennes, P. G. Statistics of macromolecular solutions trapped in small pores. *J. Phys.* **1977**, *38*, 85–93.

(9) Brochard, F.; de Gennes, P. G. Dynamics of confined polymer chains. *J. Chem. Phys.* **1977**, *67*, 52–56.

(10) Wang, Y.; Tree, D. R.; Dorfman, K. D. Simulation of DNA extension in nanochannels. *Macromolecules* **2011**, *44*, 6594–6604.

(11) Muralidhar, A.; Dorfman, K. D. Kirkwood diffusivity of long semiflexible chains in nanochannel confinement. *Macromolecules* **2015**, *48*, 2829–2839.

(12) Gupta, D.; Bhandari, A. B.; Dorfman, K. D. Evaluation of blob theory for the diffusion of DNA in nanochannels. *Macromolecules* **2018**, *51*, 1748–1755.

(13) Dai, L.; Tree, D. R.; van der Maarel, J. R. C.; Dorfman, K. D.; Doyle, P. S. Revisiting blob theory for DNA diffusivity in slitlike confinement. *Phys. Rev. Lett.* **2013**, *110*, 168105.

(14) Amin, S.; Khorshid, A.; Zeng, L.; Zimny, P.; Reisner, W. A nanofluidic knot factory based on compression of single DNA in nanochannels. *Nat. Commun.* **2018**, *9*, 1506.

(15) Suma, A.; Orlandini, E.; Micheletti, C. Knotting dynamics of DNA chains of different length confined in nanochannels. *J. Phys: Condens. Matter* **2015**, *27*, 354102.

(16) Tubiana, L.; Rosa, A.; Fragiacomo, F.; Micheletti, C. Spontaneous knotting and unknotting of flexible linear polymers: Equilibrium and kinetic aspects. *Macromolecules* **2013**, *46*, 3669–3678.

(17) Klotz, A. R.; Soh, B. W.; Doyle, P. S. Motion of knots in DNA stretched by elongational fields. *Phys. Rev. Lett.* **2018**, *120*, 188003.

(18) Ma, Z.; Dorfman, K. D. Diffusion of knots along DNA confined in nanochannels. *Macromolecules* **2020**, *53*, 6461–6468.

(19) Kundukad, B.; Yan, J.; Doyle, P. S. Effect of YOYO-1 on the mechanical properties of DNA. *Soft Matter* **2014**, *10*, 9721–9728.

(20) Günther, K.; Mertig, M.; Seidel, R. Mechanical and structural properties of YOYO-1 complexed DNA. *Nucleic Acids Res.* **2010**, *38*, 6526–6532.

(21) Gupta, D.; Sheats, J.; Muralidhar, A.; Miller, J. J.; Huang, D. E.; Mahshid, S.; Dorfman, K. D.; Reisner, W. Mixed confinement regimes during equilibrium confinement spectroscopy of DNA. *J. Chem. Phys.* **2014**, *140*, 214901.

(22) See `http://microfluidics.stanford.edu/download/CalcEquilibrium_LoC_v1p1.m` for the program for equilibrium reaction calculations.

(23) Persson, F.; Tegenfeldt, J. O. DNA in nanochannels—directly visualizing genomic information. *Chem. Soc. Rev.* **2010**, *39*, 985–999.

(24) Reisner, W.; Morton, K. J.; Riehn, R.; Wang, Y. M.; Yu, Z.; Rosen, M.; Sturm, J. C.; Chou, S. Y.; Frey, E.; Austin, R. H. Statics and dynamics of single DNA molecules confined in nanochannels. *Phys. Rev. Lett.* **2005**, *94*, 196101.

(25) Tegenfeldt, J. O.; Prinz, C.; Cao, H.; Chou, S.; Reisner, W. W.; Riehn, R.; Wang, Y. M.; Cox, E. C.; Sturm, J. C.; Silberzan, P.; Austin, R. H. The dynamics of genomic-length DNA molecules in 100-nm channels. *Proc. Natl. Acad. Sci. U.S.A.* **2004**, *101*, 10979–10983.

(26) Strychalski, E. A.; Levy, S. L.; Craighead, H. G. Diffusion of DNA in nanoslits. *Macromolecules* **2008**, *41*, 7716–7721.

(27) Akerman, B.; Tuite, E. Single- and double-strand photocleavage of DNA by YO, YOYO and TOTO. *Nucleic Acids Res.* **1996**, *24*, 1080–1090.

(28) York, D.; Evensen, N. M.; Martínez, M. L.; De Basabe Delgado, J. Unified equations for the slope, intercept, and standard errors of the best straight line. *Am. J. Phys.* **2004**, *72*, 367–375.

(29) Bhandari, A. B.; Reifenberger, J. G.; Chuang, H.-M.; Cao, H.; Dorfman, K. D. Measuring the wall depletion length of nanoconfined DNA. *J. Chem. Phys.* **2018**, *149*, 104901.

(30) Gupta, D.; Miller, J. J.; Muralidhar, A.; Mahshid, S.; Reisner, W.; Dorfman, K. D. Experimental evidence of weak excluded volume effects for nanochannel confined DNA. *ACS Macro Lett.* **2015**, *4*, 759–763.

(31) Dai, L.; van der Maarel, J.; Doyle, P. S. Extended de Gennes regime of DNA confined in a nanochannel. *Macromolecules* **2014**, *47*, 2445–2450.

(32) Werner, E.; Mehlig, B. Confined polymers in the extended de Gennes regime. *Phys. Rev. E* **2014**, *90*, 062602.

(33) Davison, P. F. The effect of hydrodynamic shear on the deoxyribonucleic acid from T2 and T4 bacteriophages. *Proc. Natl. Acad. Sci. U.S.A.* **1959**, *45*, 1560–1568.

(34) Reifenberger, J. G.; Cao, H.; Dorfman, K. D. Odijk excluded volume interaction during the unfolding of DNA confined in a nanochannel. *Macromolecules* **2018**, *51*, 1172-1180.

(35) Levy, S. L.; Mannion, J. T.; Cheng, J.; Reccius, C. H.; Craighead, H. G. Entropic unfolding of DNA molecules in nanofluidic channels. *Nano Lett.* **2008**, *8*, 3839-3844.

(36) Bao, X. R.; Lee, H. J.; Quake, S. R. Behavior of complex knots in single DNA molecules. *Phys. Rev. Lett.* **2003**, *91*, 265506.

(37) Grosberg, A. Y.; Rabin, Y. Metastable tight knots in a wormlike polymer. *Phys. Rev. Lett.* **2007**, *99*, 217801.

(38) Mavrovouniotis, G. M.; Brenner, H. Hindered sedimentation, diffusion, and dispersion coefficients for brownian spheres in circular cylindrical pores. *J. Colloid Interface Sci.* **1988**, *124*, 269–283.

(39) Dai, L.; Renner, C. B.; Doyle, P. S. Metastable knots in confined semiflexible chains. *Macromolecules* **2015**, *48*, 2812–2818.

(40) Tree, D. R.; Wang, Y.; Dorfman, K. D. Mobility of a semiflexible chain confined in a nanochannel. *Phys. Rev. Lett.* **2012**, *108*, 228105.

(41) Hernández-Ortiz, J. P.; de Pablo, J. J.; Graham, M. D. Fast computation of many-particle hydrodynamic and electrostatic interactions in a confined geometry. *Phys. Rev. Lett.* **2007**, *98*, 140602.

(42) Huang, L.; Makarov, D. E. Langevin dynamics simulations of the diffusion of molecular knots in tensioned polymer chains. *J. Phys. Chem. A* **2007**, *111*, 10338–10344.

(43) Matthews, R.; Louis, A. A.; Yeomans, J. M. Effect of topology on dynamics of knots in polymers under tension. *Europhys. Lett.* **2010**, *89*, 20001.

(44) Narsimhan, V.; Renner, C. B.; Doyle, P. S. Jamming of knots along a tensioned chain. *ACS Macro Lett.* **2016**, *5*, 123–127.

(45) Dai, L.; Doyle, P. S. Universal knot spectra for confined polymers. *Macromolecules* **2018**, *51*, 6327–6333.

(46) Vandans, O.; Yang, K.; Wu, Z.; Dai, L. Identifying knot types of polymer conformations by machine learning. *Phys. Rev. E* **2020**, *101*, 022502.

(47) Vologodskii, A. Brownian dynamics simulation of knot diffusion along a stretched DNA molecule. *Biophys. J.* **2006**, *90*, 1594–1597.

(48) Micheletti, C.; Orlandini, E. Knotting and unknotting dynamics of DNA strands in nanochannels. *ACS Macro Lett.* **2014**, *3*, 876–880.

Supporting Information for "Diffusion of Knotted DNA Molecules in Nanochannels in the Extended de Gennes Regime"

Zixue Ma and Kevin D. Dorfman*

Department of Chemical Engineering and Materials Science, University of Minnesota – Twin Cities, 421 Washington Ave SE, Minneapolis, Minnesota 55455, USA

E-mail: dorfman@umn.edu

k-means clustering analysis

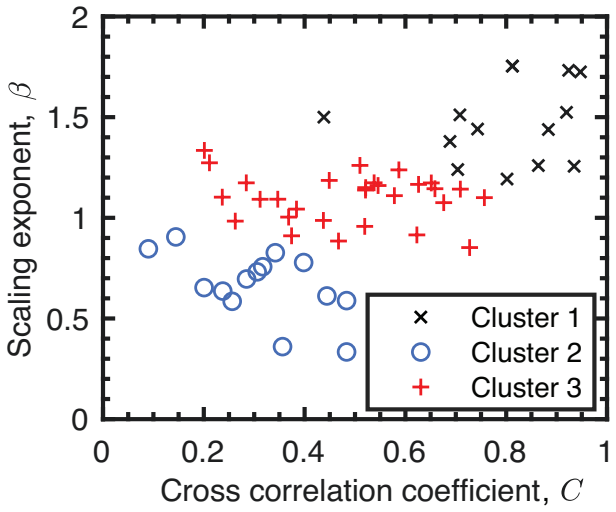

Figure S1: k-means clustering result for the data of scaling exponent, β, and average cross correlation coefficient, C, for an ensemble of T4 DNA molecules in each movie. The k-means clustering analysis partition the data into three clusters that molecules are highly correlated and superdiffusive, relatively uncorrelated, and very uncorrelated. The cluster 1 (black $\times$) is the data set of DNA molecules with high β and C values. These molecules are highly correlated with all of the other molecules within the same movie and exhibit strongly superdiffusive behavior, and were excluded from the subsequent DNA diffusion analysis. Clusters 2 (blue $\bigcirc$) is the data set of very uncorrelated molecules with relatively small beta values. The molecules in cluster 3 (red $+$) are relatively uncorrelated DNA molecules with beta values between 0.8 and 1.4. The intact T4 DNA molecules with knots formed after the compression process in cluster 2 and cluster 3 are used for DNA diffusion analysis.

Determination of upper and lower bounds

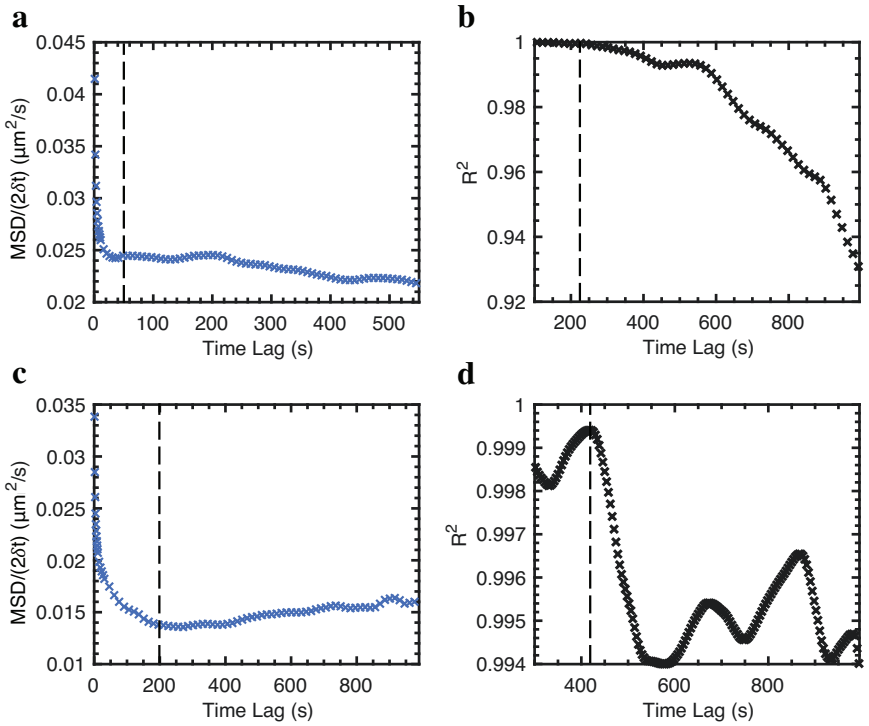

Figure S2: Determination of upper and lower bounds of the time lag used for fitting the T4 DNA chain diffusivity in nanochannels before and after knotting. (a, c) The dynamic diffusion coefficient, MSD/$2\delta t$, as a function of time lag and (b, d) the correlation coefficient, R^2, of the linear fit line Eq. 5 with different upper bounds and a fixed lower bound for unknotted DNA (a, b) and knotted DNA molecules (c, d). The MSD/$2\delta t$ curve decays continuously until the time lag of 50 s for unknotted DNA molecules and 200 s for DNA with knots. The initial decay is due to a dynamical error from the DNA motion during finite exposure time.[1] The lower bound thus is 50 s for the DNA before knotting and 200 s for the knotted DNA molecules. The upper bound for fitting the ensemble-averaged MSD data to obtain the DNA chain diffusivity, D, is determined by calculating the R^2 of the linear fit function Eq. 5 with different upper bounds and a fixed lower bound of 50 s for unknotted DNA and 200 s for knotted DNA. The R^2 curve of unknotted DNA starts to decay at the time lag of 227 s which is determined to be the upper bound for the unknotted DNA. For DNA with knots, the upper bound is 418 s, which is the point with the largest value of R^2. The lower and upper bounds are indicated by the black vertical dashed lines.

References

(1) Savin, T.; Doyle, P. S. Static and dynamic errors in particle tracking microrheology. *Biophys. J.* **2005**, *88*, 623–638.